Overview on solar, geo, and reactor neutrino experiments

L Ludhova

Institut für Kernphysik, Forschungszentrum Jülich, 52425 Jülich, Germany and RWTH Aachen University, 52062 Aachen, Germany

E-mail: `l.ludhova@fz-juelich.de`

Abstract. Neutrino physics has made a substantial progress in recent years: ranging from the discovery of new phenomena, as neutrino oscillations, up to the development of milestone experimental techniques, going, at the end, hand-in-hand. Today, we are able to do precision neutrino physics, as well as we have succeeded in using neutrinos as new tools to gain information about astrophysical objects. In spite of this enormous progress, many fundamental questions remain unanswered. This contribution concentrates on low-energy MeV neutrinos emitted from our Sun, along the radioactive decays inside the Earth (geoneutrinos), and reactor neutrinos. For each of these three fields, the present-day motivation, open questions, as well as the latest experimental results and future perspectives are discussed.

1. Introduction

Neutrinos interact with matter only through the weak interactions and thus, their probability to interact is small. This makes their detection extremely challenging: imagine, from billions of solar neutrinos crossing every second every cm^2 of the Earth's surface, it is only at the order of 200 that would eventually interact in 100 ton of a typical liquid scintillator target per day. Thus, neutrino detectors must have large volumes, have to be constructed from extremely radio-pure materials, and have to be shielded from cosmic radiation in underground laboratories. On the other had, thanks to this very same property of small interaction cross sections, neutrinos reach our detectors nearly unperturbed from their sources. Thus, we can use them as messengers from otherwise unreachable locations inside astronomical objects.

In spite of a huge progress of neutrino physics, there are still fundamental questions to be answered about neutrino properties. The observed mechanism of neutrino oscillations did confirm the existence of two distinct mass differences, e.g. the solar (at the order of $10^{-5}\,\mathrm{eV}^2$) and the atmospheric one (at the order of $10^{-3}\,\mathrm{eV}^2$), and thus the non-zero value of the rest mass of at least two mass eigenstates. Even if we do not know the absolute neutrino mass, the existing upper limits show us, that it is orders of magnitude smaller with respect to the masses of other fermions. We do not know the mechanism generating neutrino mass, whether their character is Majorana or Dirac. We do not know whether the third mass eigenstate m_3 is heavier or lighter that the mass eigenstates m_1 and m_2, that is, whether the mass ordering is normal or inverted, respectively. We have measured the three mixing angles $\theta_{12} \sim 45°$, $\theta_{13} \sim 9°$, and $\theta_{23} \sim 33°$ parameterizing the neutrino mixing matrix that relates the neutrino mass and flavor eigenstates. The value of the CP-violating phase, also entering in the parameterization
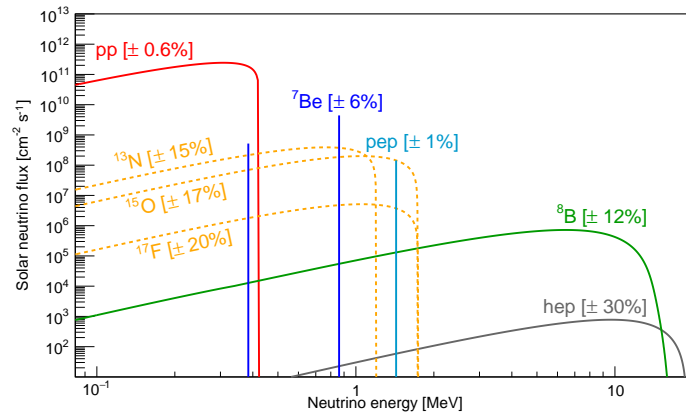
Figure 1. Expected energy spectrum of solar neutrinos from the pp and CNO nuclear fusion sequences. The flux (vertical scale) is given in units of $\text{cm}^{-2}\,\text{s}^{-1}\,\text{MeV}^{-1}$ for continuum sources and in $\text{cm}^{-2}\,\text{s}^{-1}$ for mono-energetic sources. From [1] and references therein.

of this matrix, is not yet known. However, the latest results hint at their non-zero value and this could, possibly, solve the mystery of the matter-antimatter asymmetry in the present-day Universe.

In this contribution, we concentrate on the results from the experiments measuring low-energy MeV neutrinos emitted from our Sun, along the radioactive decays inside the Earth (geoneutrinos), and reactor anti-neutrinos.

2. Solar neutrinos

Our Sun is powered by nuclear fusion reactions occurring in the hot solar core and solar neutrinos are the only direct probe about these processes. The so-called pp fusion chain is providing about 99% of solar energy. The Carbon-Nitrogen-Oxygen catalyzed fusion cycle (CNO) has not yet been observed, but is believed to be a sub-dominant process in the Sun, while a dominant energy-production mechanism in heavier stars. Figure 1 illustrates the energy spectra of emitted neutrinos, as predicted by the Standard Solar Model (SSM).

Solar neutrinos are emitted as electron flavor neutrinos but due to the process of neutrino oscillations, strongly influenced by the dense solar matter (the so-called MSW effect [2]), arrive on the Earth as a mixture of all flavors, with the relative proportions dependent on neutrino energy. Solar neutrinos are detected via the elastic scattering off electrons that is sensitive to all neutrino flavors. The scattered electrons are then causing the emission of either scintillation light in organic liquid scintillators or Cherenkov light in water.

Recently, Borexino collaboration has reported a comprehensive measurement of the pp-chain neutrinos [1], based on the Phase-II data (December 2011 to May 2016). Borexino is a 280 ton liquid scintillator detector placed at Laboratori Nazionali del Gran Sasso in Italy. It is characterized by unprecedented radio-purity. With respect to the previous results [3–5], improvements in the radio-purity of the detector as well as in the analysis strategies have been made. Borexino has reported the precision measurement of ^7Be neutrinos (2.7%), improved measurement of pp neutrinos, and, for the first time, more than 5σ confirmation of the existence of pep neutrinos. The corresponding analysis has been performed by a multi-variate fit of the energy spectra in the energy range from 0.19 to 2.93 MeV (an example is shown in the left part of Fig. 2), including pulse-shape and radial distributions of events. By choice, in order not to make any assumptions on the oscillated ^8B neutrino energy spectrum, its rates in the energy intervals 3.2 to 5.7 MeV and 5.7 to 16 MeV, have been obtained by radial fits of the events in
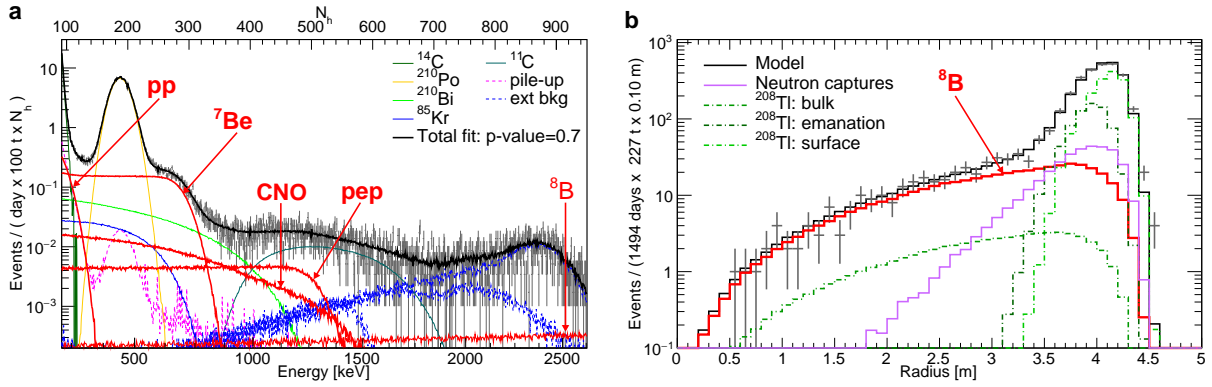
Figure 2. Borexino spectra [1] used to extract pp-chain solar-neutrino rates. Left: energy spectrum with the best fit including pp, ^{7}Be, and pep solar neutrinos; ^{8}B and CNO neutrinos are fixed to their SSM expected values. Several background components are also shown. Right: radial distribution of events in the 3.2 to 5.7 MeV energy interval used to extract the ^{8}B neutrino rates.

the respective energy intervals (right-hand part of Fig. 2). These measurements provide a direct determination of the relative intensity of the two primary terminations of the pp chain (pp-I and pp-II) and an indication that the temperature profile in the Sun is more compatible with Standard Solar Models that assume high surface metallicity [6]. Assuming solar neutrino fluxes predicted by SSM, Borexino also determines the survival probability of solar electron-flavor neutrinos P_{ee} at different energies (Fig. 3), thus probing simultaneously the neutrino flavor-conversion paradigm, both in vacuum- and in matter-dominated regimes. Borexino is currently in the quest for measurement of CNO solar neutrinos. This would require an independent estimation of the ^{210}Bi contamination of liquid scintillator, in order to break the degeneracy of the respective spectral shapes. After the thermal stabilization of the detector, this might be possible through evaluation of the easily-tagged α-decays of ^{210}Po.

SuperKamiokande (SuperK) is a water-Cherenkov detector containing 50 kton of ultra-pure water, placed in Kamioka mine in Japan. With respect to scintillator detectors, the main advantage, apart the extra-large volume, is the sensitivity to the direction of incoming neutrino, that opens-up a possibility for background rejection. The main disadvantage, however, is smaller light yield, consequently worse resolution, and few-MeV energy threshold. Thus, SuperK is able to measure only ^{8}B solar neutrinos. SuperK contributed to the discovery of solar neutrino flavor transformation and also today with about 56,000 detected solar neutrinos determines the precision of the measurement of the θ_{12} mixing angle [10]. SuperK phase IV started in September 2008 and is characterized by the lowest energy threshold of 3.2 MeV. These data is well suited to test the so-called transition region where the survival probability curve changes from the vacuum- to matter-dominated region [8–10]. This is particularly important in a view of the fact that some new physics could influence the exact shape of this transition region, as for example the Non-Standard neutrino Interactions (NSI) [7]. As it can be seen in Fig. 4, the energy dependent P_{ee} of ^{8}B neutrinos, shown as the red area, does not show the expected upturn from the vacuum- to matter-dominated regimes. In addition, the best fit value of the Δm_{12}^2 is in ca. 2σ tension with the KamLAND best fit. The final publication of the SuperK-IV data is under preparation. SuperK was in refurbishment in 2018, is being filled in 2019, and will be loaded with Gd in 2020, with the main aim to detect Diffuse SuperNovae Background (DSNB) neutrinos.
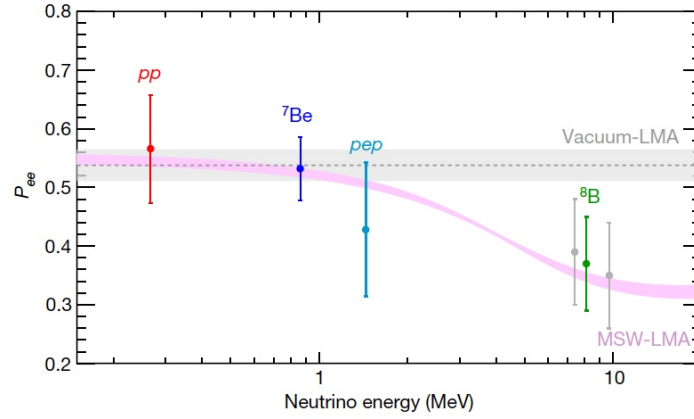
Figure 3. Electron neutrino survival probability P_{ee} as a function of neutrino energy [1]. The pink band is the MSW-LMA prediction (LMA = Large Mixing Angle neutrino oscillations solution). The grey band is the vacuum-LMA case, excluded with 98.2% C.L. Data points represent the Borexino results, with errors including experimental and theoretical uncertainties. ^{8}B and *pp* data points are set at the mean energy of neutrinos that produce scattered electrons in the energy intervals of respective analyses.
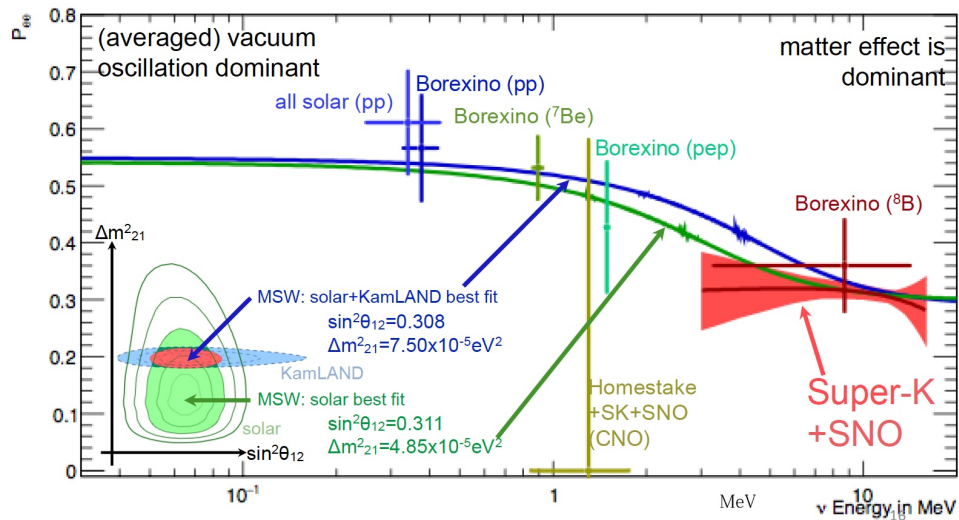

Figure 4. SuperKamiokande results on electron-flavour neutrino survival probability and oscillation parameters θ_{12} and Δm^2_{12} [9]. Please note, that Borexino data points shown on the plot do not include the new results from [1] given in Fig. 3.

3. Geoneutrinos

Geoneutrinos are electron-flavor antineutrinos emitted in the β decays of long-lived radioactive elements, called also *the heat producing elements* (HPE): along the decay chains of ^{238}U and ^{232}Th and in the ^{40}K decay. The main aim of geoneutrino studies is to determine the Earth's radiogenic heat, especially the unknown contribution from the mantle. The mantle composition is quite unknown with respect to the better-known crustal composition. Knowing the mass/abundances of HPE, the radiogenic heat is directly determined. The geoneutrino studies are, however, complicated through an unknown distribution of HPE, on which depends both the geoneutrino signal prediction as well as the final interpretation of the measured geoneutrino flux.
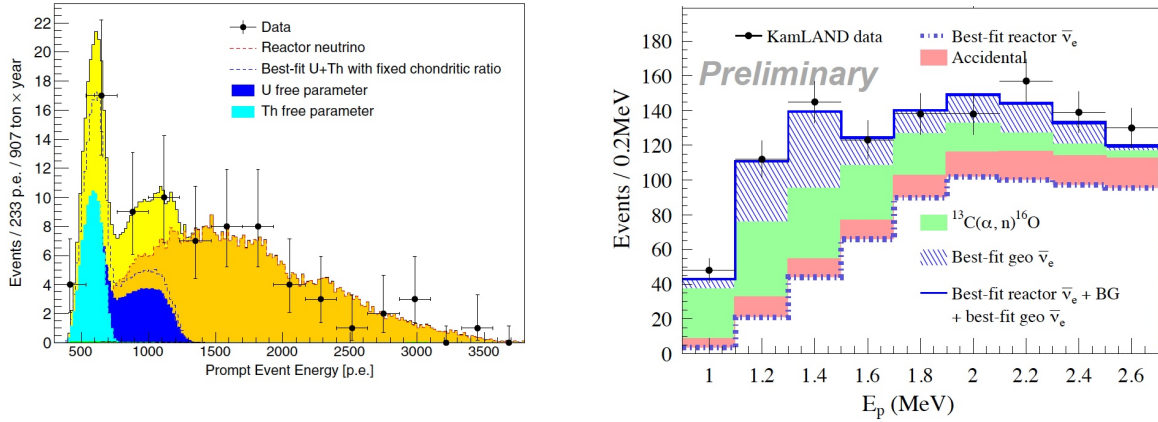
Figure 5. Left: prompt light yield spectrum (1 MeV corresponds to $\sim$500 photoelectrons) of 77 antineutrino candidates measured by Borexino and the best fit [13]. The non-antineutrino background is not visible and corresponds to less than 1 event. Right: preliminary geoneutrino analysis of KamLAND from 2016 [12] shown until the end-point of geoneutrino spectrum.

Electron antineutrinos, as it is the case of geoneutrinos, are detected by the inverse-beta decay (IBD) reaction

$$\bar{\nu}_e + p \rightarrow e^+ + n, \tag{1}$$

that is a charge-current interaction and is sensitive only to electron flavor neutrinos. Organic liquid scintillators are used as proton-rich targets. Only antineutrinos with energies above 1.8 MeV, the kinematic threshold of this interaction, can be detected: leaving ^{40}K geoneutrinos unreachable to present day detection techniques. Reactor neutrinos, also electron flavor antineutrinos, are detected by the very same process and represent an irreducible background in geoneutrino measurements. The IBD interaction provides, however, a powerful tool to suppress other types of backgrounds, thanks to a possibility to require a space and time coincidence between the prompt signal and the delayed one. The positron comes quickly to rest and then annihilates emitting two 511 keV γ-rays, yielding a *prompt event*. The visible energy E_{prompt} is directly correlated with the incident antineutrino energy $E_{\bar{\nu}_e}$: $E_{prompt} = E_{\bar{\nu}_e} - 0.784$ MeV. The neutron, also produced in IBD reaction, keeps initially the information about the incident $\bar{\nu}_e$ direction. Unfortunately, it is typically captured on protons only after a long thermalization time with $\tau = 200$ - $250\,\mu$s (depending on scintillator), during which this information is mostly lost. When the thermalized neutron is captured on proton, a 2.22 MeV de-excitation γ-ray is emitted, providing a coincident *delayed event*.

Today, only two experiments succeeded to measure geoneutrinos: KamLAND in Kamioka mine in Japan and Borexino in Italy. KamLAND contains about 1 kton of liquid scintillator and was originally constructed to measure reactor neutrino oscillations. The latest geoneutrino result published by KamLAND, 116^{+28}_{-27} geoneutrinos detected with 4.9×10^{32} target-proton $\times$ year exposure, is from 2013 [11]. It includes the three different periods: Period 1 (2002-2007) before the liquid scintillator purification with large amount of reactor, accidental, and (α, n) backgrounds; Period 2 (2009-2011) after the purification, with the non-antineutrino background strongly suppressed, and Period 3, after the 2011 Fukushima accident, with further strong reduction of reactor antineutrino background. KamLAND has released a preliminary result in 2016 on a conference talk [12] including the low-reactor background data until 2016. The best fit yielded 164^{+28}_{-25} geoneutrinos with 6.39×10^{32} target-proton $\times$ year exposure and is shown in right-hand side of Fig. 5.
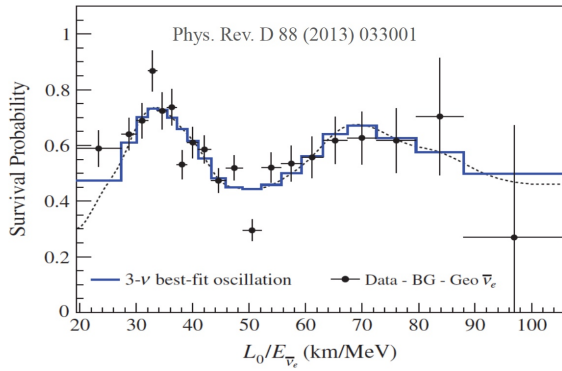
Figure 6. Ratio of the reactor antineutrino spectrum observed by KamLAND to the expectation for no-oscillation versus the ratio of the baseline $L_0 = 180\,\mathrm{km}$ and neutrino energy [11]. In blue is shown the best fit assuming 3-neutrino flavor oscillation.
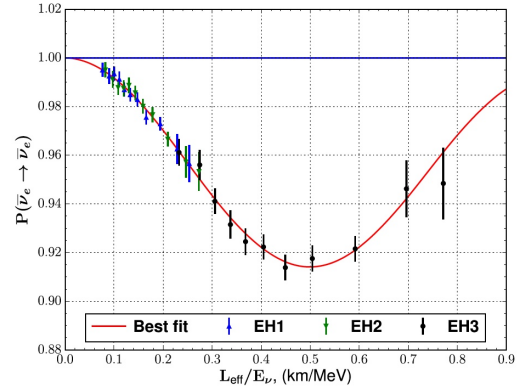

Figure 7. Reactor antineutrino spectral distortion measured by Daya Bay [20], displayed as the oscillation survival probability versus the ratio of the effective baseline and neutrino energy. The amplitude of the disappearance is proportional to $\sin^2 2\theta_{13}$.

Borexino provided the latest update in 2015 [13], as demonstrated in left-hand side of Fig. 5. Within the exposure of $(5.5 \pm 0.3) \times 10^{31}$ target-proton × year, $23.7^{+6.5}_{-5.7}(\text{stat})^{+0.9}_{-0.6}(\text{sys})$ geoneutrino events have been detected. The null observation of geoneutrinos has a probability of 3.6×10^{-9} (5.9σ). A geoneutrino signal from the mantle is obtained at 98% confidence level. The radiogenic heat production for U and Th from the present best-fit result is restricted to the range 23 to 36 TW, taking into account the uncertainty on the distribution of HPE inside the Earth.

The existing geoneutrino measurements are in agreement with expectations based on geological models. This is a remarkable achievement of both geosciences, being able to model the composition of the deep layers of our planet, as well as of neutrino physics, being able to measure the faint geoneutrino signal. However, due to the large error of the existing geoneutrino measurements, it is not possible to distinguish among different geological models. In the near future, an update is expected from KamLAND, including more low-background data. Borexino is preparing a new update with improved analysis with the expected precision of about 20%. Future experiments SNO+ [14], JUNO [15], and Jinping [16] have geoneutrinos among their scientific goals. A real breakthrough would come with the proposed Hanohano [17] project in Hawaii: placed underwater on a thin, HPE-depleted oceanic crust, where the mantle contribution to the total geoneutrino flux would be dominant.

4. Reactor neutrinos

Nuclear reactors are the strongest human-made source of neutrinos. Reactor neutrinos are electron anti-neutrinos originating from the fission of $^{235}\mathrm{U}$, $^{239}\mathrm{Pu}$, $^{238}\mathrm{U}$, and $^{241}\mathrm{Pu}$ isotopes. They are detected through the same charge-current IBD interaction, as in Eq. 1. Considering the energy-dependent cross section of this interaction, the reactor-neutrinos energy spectrum peaks at about 3-4 MeV and has an end point at about 9-10 MeV.

Reactor antineutrinos played an important role in neutrino physics since very beginning. The existence of neutrino was in fact experimentally confirmed in a famous experiment of Reines and Cowan in 1956 [18], through the detection of reactor neutrinos. Even today, they play an important role in neutrino physics. The physics goals of these experiments strongly depend on the distance between the reactor and the detector.

KamLAND experiment, with its baseline $L \sim 200\,\mathrm{km}$, is positioned in the 2nd minimum of the "solar oscillation", e.g. of the term $\sin^2\left(\frac{\Delta m_{12}^2 L}{4E}\right)$ entering the survival probability of reactor neutrinos. KamLAND has provided the first evidence of Δm_{12}^2 driven oscillations [19] and has an optimized sensitivity to measure the solar mass splitting Δm_{12}^2, as it is shown in Fig. 6.

The baseline of about 1-2 km is optimal for observing the disappearance due to Δm_{ee}^2 driven oscillations, which amplitude is given by $\sin^2 2\theta_{13}$. The three experiments of this type have indeed measured the θ_{13} mixing angle: Daya Bay [20], Double Chooz [21], and RENO [22]. Figure 7 shows the spectral distortion measured by Daya Bay.

Daya Bay provided also the highest statistics measurement of the reactor antineutrino spectrum through the detection of 1.2 million IBD interactions [23]. It is shown in Fig. 8: when compared, as in the middle panel, to the Huber-Mueller prediction [24, 25], one observes an integral deficit of about 6% of events as well as an excess of events in region 4-6 MeV. These features were consistently observed also by Double Chooz [21] and RENO [22]. A possible explanation of the observed deficit and the so called reactor anomaly [27] could be a possible overestimation of the IBD yield of ^{235}U by 7.8%, based on the Daya Bay observation of the evolution of the shape of the reactor spectrum as a function of the composition of the reactor [26]. The origin of the observed structure at 4-6 MeV is currently not understood.

The very-short-baseline reactor neutrino experiments, e.g. with the baseline at the order of few meters, are testing another hypothesis that could explain the observed deficit of reactor neutrinos [27]. This could be an active oscillation to a light sterile neutrino with $\Delta m^2 \sim 1\,\mathrm{eV}^2$. Disappearance of MeV neutrinos at several meters baseline is incompatible with the 3-neutrino picture. Several experiments around the world are now taking data and the first results were published. These mostly exclude the best fit of the so-called reactor anomaly and are fully compatible with the 3-neutrino picture. These include the results of NEOS [28] and DANSS [29], see Fig. 4, as well as those of PROSPECT [30] and Stereo [31]. Neutrino-4 [32] is the only experiment claiming oscillation with $\Delta m^2 \sim 7.3\,\mathrm{eV}^2$, that is however in tension with other experiments.

References

[1] Agostini M et al. (Borexino Coll.) 2018 *Nature* **562** 496.
[2] Pontecorvo B 1967 *Zh. Eksp. Teor. Fiz.* **53** 1717; Wolfenstein L 1978 *Phys. Rev. D* **17** 2369; Mikheyev S and Smirnov A 1985 *Sov. J. Nucl. Phys.* **42** 913.
[3] Bellini G et al. (Borexino Coll.) 2014 *Phys. Rev. D* **89** 112007.
[4] Bellini G et al. (Borexino Coll.) 2014 *Nature* **512** 383.
[5] Bellini G et al. (Borexino Coll.) 2010 *Phys. Rev. D* **82** 033006.
[6] Vinyoles N et al. 2017 *Astrop. Phys. J* **835** 202.
[7] Minakata Y and Peña-Garay C 2012 *Adv. High En. Phys.* **2012** ID 349686.
[8] Abe K et al. (Super-Kamiokande Coll.) 2016 *Phys. Rev. D* 94 052010.
[9] Ikeda M for Super-Kamiokande Col., talk at Neutrino 2018 conference, June 4-9, 2018, Heidelberg, Germany.
[10] Smy M for Super-Kamiokande Coll., talk at NNN 2018 conference, November 1-3, 2018, Vancouver, Canada.
[11] Gando A et al. (KamLAND Coll.) 2013 *Phys. Rev. D* **88** 033001.
[12] Watanabe H for KamLAND Coll., talk at International Workshop: Neutrino Research and Thermal Evolution of the Earth, October 25-27, 2016, Sendai, Japan.
[13] Agostini M et al. (Borexino Coll.) 2015 *Phys. Rev. D* **92** 031101 (R).
[14] Chen M 2016 *Earth, Moon and Planets* **99** 221.
[15] An F. et al. (JUNO Coll.) 2016 *J. Phys. G: Nucl. Part. Phys.* **43** 030401.
[16] Beacom J F et al. (Jinping Coll.) 2017 *Chin. Phys. C* **41** 023002.
[17] Learned J G, Dye S T, and Pakvasa S 2008, arXiv: 0810.4975
[18] Cowan C L et al. 1956 *Science* **24** 103.
[19] Eguchi K et al. (KamLAND Coll.) 2003 *Phys. Rev. Lett.* **90** 021802.
[20] An F P et al. (Day Bay Coll.) 2017 *Phys. Rev. D* **95** 072006.
[21] Abe Y et al. (Double Chooz Coll.) 2016 *JHEP* **01** 163.
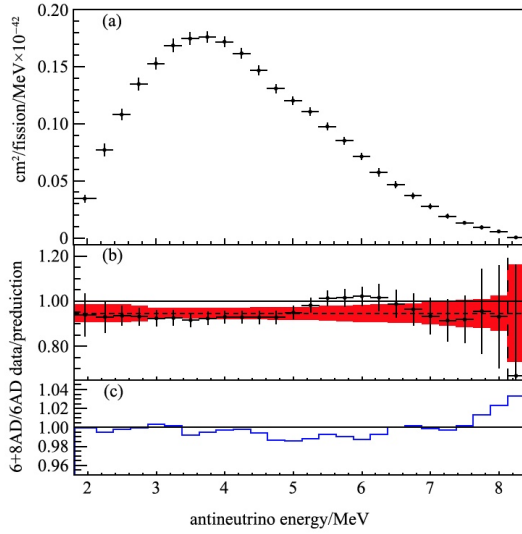[22] Choi J H et al. (RENO Coll.) 2016 *Phys. Rev. Lett.* **116** 211801.

Figure 8. The high statistics reactor antineutrino spectrum measured by Daya Bay [23]. The middle panel shows the ratio of the spectrum with respect to the expectation according to Mueller at al. [24].
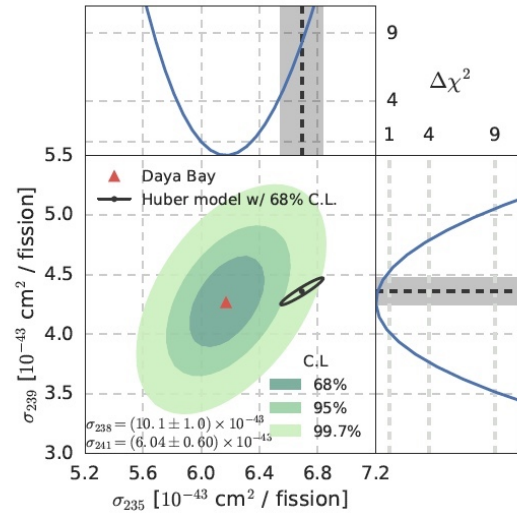

Figure 9. Combined measurement of ^{235}U and ^{239}Pu IBD yields per fission, σ_{235} and σ_{239}, measured by Daya Bay [26] and compared to Huber-Mueller [24, 25] prediction shown in black.
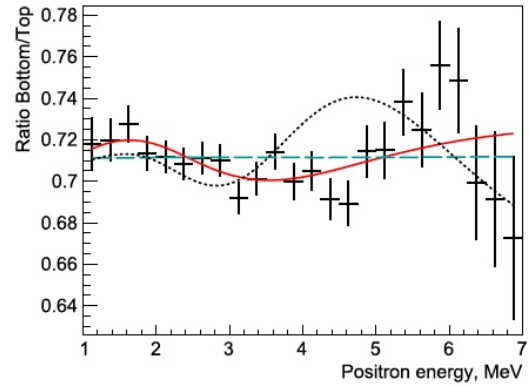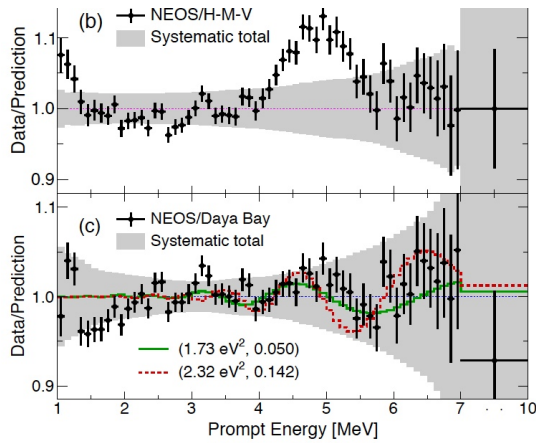

Figure 10. First results from very-short-baseline reactor neutrino experiments testing the hypotheses of a light sterile neutrino through the search for neutrino oscillations not compatible with 3-neutrino picture. Left: results from NEOS [28], comparing the measured positron spectral shape to: Huber-Mueller [24, 25] prediction (top, note the clear excess at 4-6 MeV) and Daya Bay spectrum (bottom). Right: ratio of the positron energy spectra measured at the bottom and top detectors of DANSS [29].

[23] An F P et al. (Day Bay Coll.) 2017 *Chin. Phys. C* **41** 013002.
[24] Mueller A et al. 2011 *Phys. Rev. C* **83** 054615.
[25] Huber P 2011 *Phys. Rev. C* **84** (2011) 024617.
[26] An F P et al. (Day Bay Coll.) 2017 *Phys. Rev. Lett.* **118** 251801.
[27] Mention G et al. 2011 *Phys. Rev. D* **83** 073006.
[28] Ko Y J et al. (NEOS Coll.) 2017 *Phys. Rev. Lett.* **118** 121802.
[29] Alekseev I et al. (DANSS Coll.) 2018 *Phys. Lett. B* **787** 56.

[30] Ashenfelter J et al. (PROSPECT Coll.) 2018 *Phys. Rev. Lett.* **121** 251802.
[31] Almazan H et al. (Stereo Coll. 2018 *Phys. Rev. Lett.* **121** 161801.
[32] Serebrov A P et al. (Neutrino-4 Coll.) 2019 *Jetp Lett.* **10** 1134.